

In medium properties of strange Hadrons

E. Oset

Universidad de Valencia - IFIC

Unitarized Chiral Perturbation Theory

Skillful combination of the information of the Chiral Lagrangians and unitarity in coupled channels.

- Pioneering work of *Kaiser, Siegel, Waas, Weise 95-97* using Lipmann-Schwinger eq. and input from Chiral Lagrangians as potential.

- Subsequent work

- Inverse Amplitude Method (IAM) → $\left\{ \begin{array}{l} \text{Truong} \\ \text{Dobado, Peláez '97} \\ \text{Oller, E.O., Peláez '98} \end{array} \right.$

- (N/D) method → $\left\{ \begin{array}{l} \text{Oller, E.O. '99} \\ \text{Oller, Meissner '01} \end{array} \right.$

- Bethe-Salpeter eq. → $\left\{ \begin{array}{l} \text{Oller, E.O. '97} \\ \text{Nieves, Ruiz-Arriola '00} \end{array} \right.$

Hosaka, Hyodo ; Lutz, Kolomeitsev ; Borasoy, Nisler, Weise

- Applications → $\left\{ \begin{array}{l} \text{Ramos, Vicente, Marco, Parreño, Toki, Hirenzaki} \\ \text{Hosaka, Oka, Nacher, Palomar, Jido, Inoue, Roca} \\ \text{Cabrera, Okumura, Takahashi, Mizobe, Chiang} \\ \text{Kamalov, Bennhold, Hernández, García Recio} \end{array} \right.$

Meson-Baryon interaction

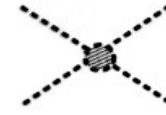
$$\mathcal{L}_1^{(B)} = \langle \bar{B} i \gamma^\mu \nabla_\mu B \rangle - M_B \langle \bar{B} B \rangle + \frac{D}{2} \langle \bar{B} \gamma^\mu \gamma_5 \{u_\mu, B\} \rangle + \frac{F}{2} \langle \bar{B} \gamma^\mu \gamma_5 [u_\mu, B] \rangle$$

$$u_\mu = i u^\dagger \partial_\mu U u^\dagger \quad ; \quad u^2 = U = e^{i \frac{\sqrt{2}}{f} \Phi}$$

$$\nabla_\mu B = \partial_\mu B + [P_\mu, B] \quad ; \quad P_\mu = \frac{1}{2} (u^\dagger \partial_\mu u + u \partial_\mu u^\dagger)$$

$$B(x) \equiv \begin{pmatrix} \frac{1}{\sqrt{2}} \Sigma^0 + \frac{1}{\sqrt{6}} \Lambda^0 & \Sigma^+ & p \\ \Sigma^- & -\frac{1}{\sqrt{2}} \Sigma^0 + \frac{1}{\sqrt{6}} \Lambda^0 & n \\ \Xi^- & \Xi^0 & -\frac{2}{\sqrt{6}} \Lambda^0 \end{pmatrix}$$

$$\chi \text{ PT: (mesons)} \quad \Phi \equiv \begin{pmatrix} \frac{1}{\sqrt{2}} \pi^0 + \frac{1}{\sqrt{6}} \eta & \pi^+ & \kappa^+ \\ \pi^- & -\frac{1}{\sqrt{2}} \pi^0 + \frac{1}{\sqrt{6}} \eta & \kappa^0 \\ \kappa^- & \bar{\kappa}^0 & -\frac{2}{\sqrt{6}} \eta \end{pmatrix}$$



Successful at low energies

Problems → { Limited energy range of applicability
Cannot deal with resonances

General scheme Oller, Meissner PL '01 (meson baryon as exemple)

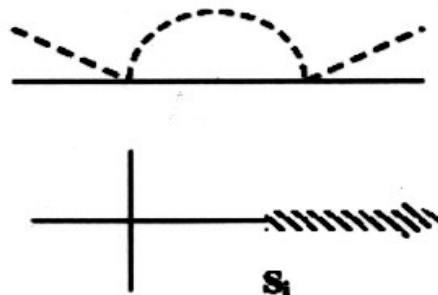
- **Unitarity** in coupled channels $\bar{K}N, \pi\Sigma, \pi\Lambda, \eta\Sigma, \eta\Lambda, K\Xi$, in $S = -1$

$$\begin{aligned} \text{Im}T_{ij} &= T_{il}\sigma_{ll}T_{lj}^* \\ \sigma_l &\equiv \sigma_{ll} \equiv \frac{2Mq_l}{8\pi\sqrt{s}} \\ \sigma &= -\text{Im}T^{-1} \end{aligned}$$

- Dispersion relation

$$\begin{aligned} T_{ij}^{-1} &= -\delta_{ij} \left\{ \hat{a}_i(s_0) + \frac{s-s_0}{\pi} \int_{s_i}^{\infty} ds' \frac{\sigma(s')_i}{(s-s')(s'-s_0)} \right\} + \\ &+ V_{ij}^{-1} \equiv -g(s)_i \delta_{ij} + V_{ij}^{-1} \end{aligned}$$

$g(s)$ accounts for the right hand cut



V accounts for local terms, pole terms and crossed dynamics. V is determined by matching the general result to the χ PT expressions (usually at one loop level)

$$g(s) = \frac{2M_i}{16\pi^2} \left\{ a_i(\mu) + \log \frac{m_i^2}{\mu^2} + \frac{M_i^2 - m_i^2 + s}{2s} \log \frac{M_i^2}{m_i^2} + \frac{q_i}{\sqrt{s}} \log \frac{m_i^2 + M_i^2 - s - 2q_i\sqrt{s}}{m_i^2 + M_i^2 - s + 2q_i\sqrt{s}} \right\}$$

μ regularization mass
 a_i subtraction constant

Inverting T^{-1} :

$$T = [1 - Vg]^{-1}V$$

Example 1: Take $V \equiv$ lowest order chiral amplitude

In meson-baryon S -wave

$$[1 - V g] T = V \rightarrow T = V + V g T$$

Bethe Salpeter eqn. with kernel V

This is the method of *E. O., Ramos '98* using cut off to regularize the loops

Oller, Meissner show equivalence of methods with

$$a_i(\mu) \simeq -2 \ln \left[1 - \sqrt{1 + \frac{m_i^2}{\mu^2}} \right];$$

μ cut off

$$a_i \simeq -2 \rightarrow \mu \simeq 630 \text{ MeV in } \bar{K}N$$

If higher order Lagrangians not well determined
then fit a_i to the data

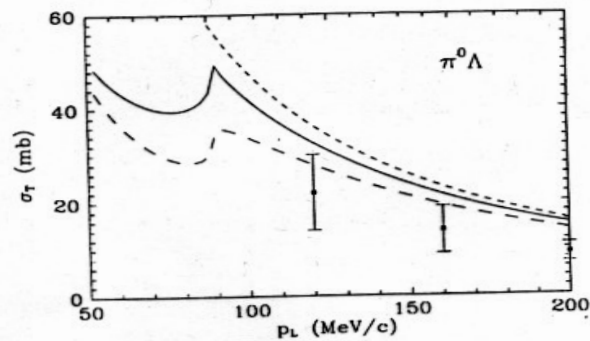
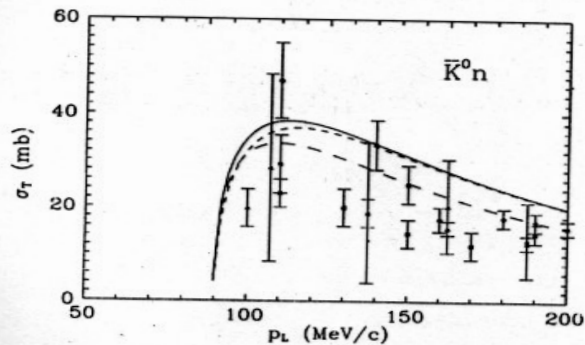
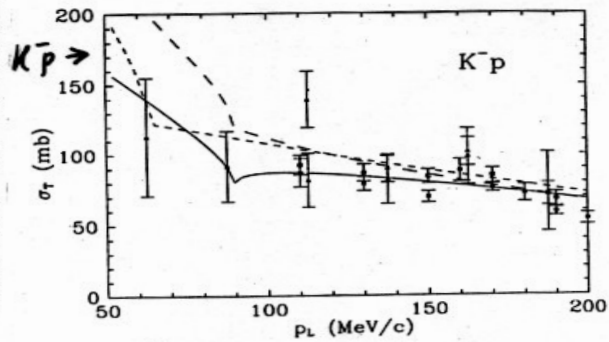
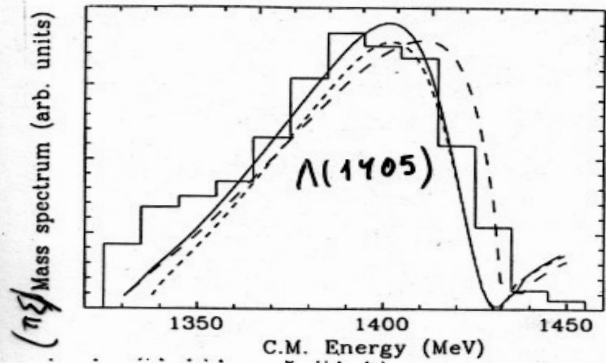
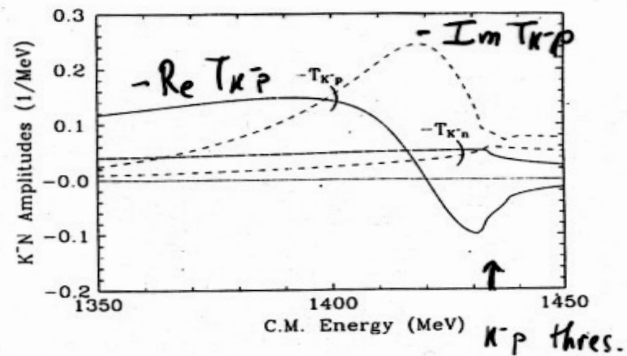
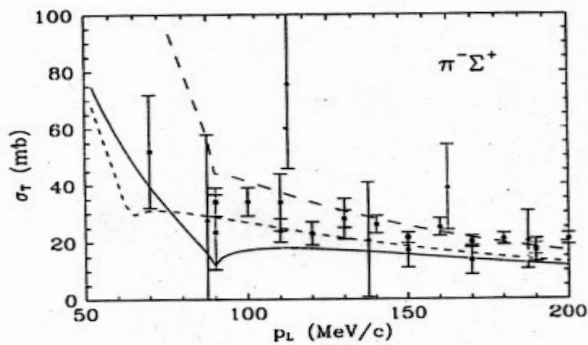
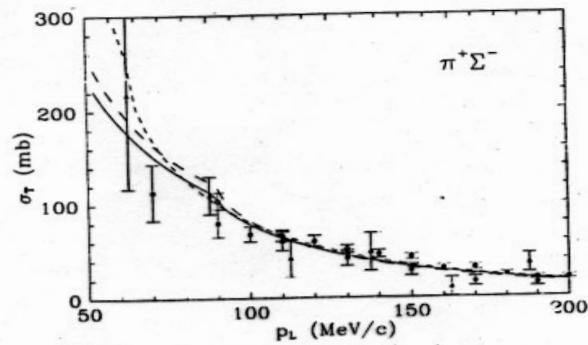
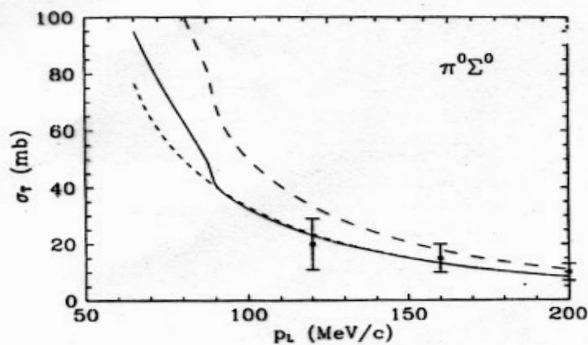


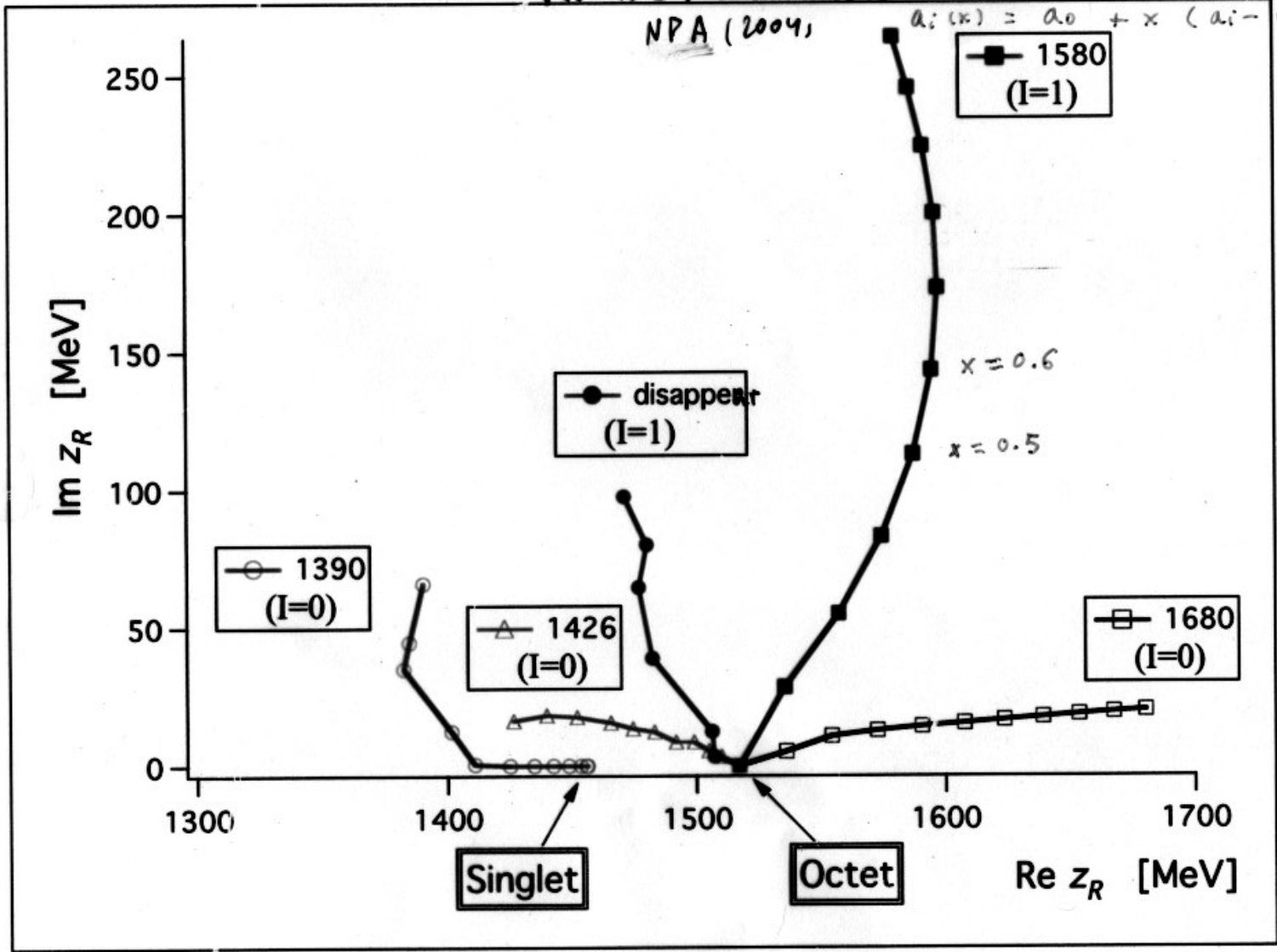
Fig. 5. Same as Fig. 3 for $K^- p \rightarrow \pi^0 \Lambda$.



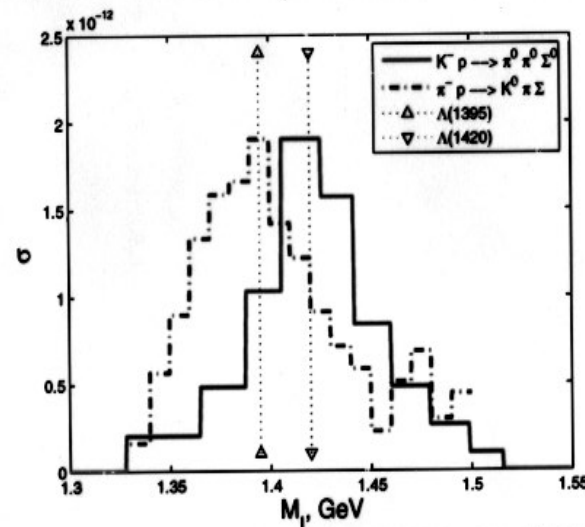
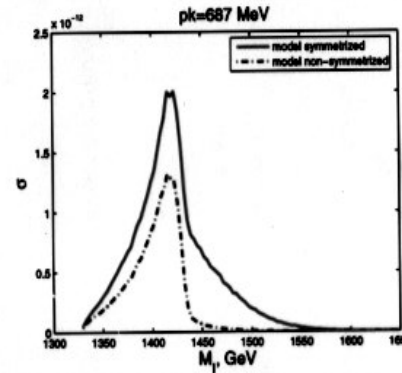
D. Jido, Oller, E.O. Ramos, U.G. Meissner
 NPA (2004)

$$M_i(x) = M_0 + x(M_i - M_0)$$

$$m_i^2(x) = m_0^2 + x(m_i^2 - m_0^2)$$

$$a_i(x) = a_0 + x(a_i - a_0)$$


Evidence for the two pole structure of the $\Lambda(1405)$



$\Gamma \approx 30 \text{ MeV}$
 $M \approx 1420 \text{ MeV}$

$\Gamma \approx 65 \text{ MeV}$
 $M \approx 1396 \text{ MeV}$

Evidence for the two pole structure of the $\Lambda(1405)$ resonance and the nature of the $\Lambda(1520)$ - p.8/11

Puri, March 2005

V. K. Magas, E. Oset and A. Ramos, **Phys. Rev. Lett.** 2005

$$\mathcal{L} = -i\bar{T}^\mu \not{D} T_\mu \quad (1)$$

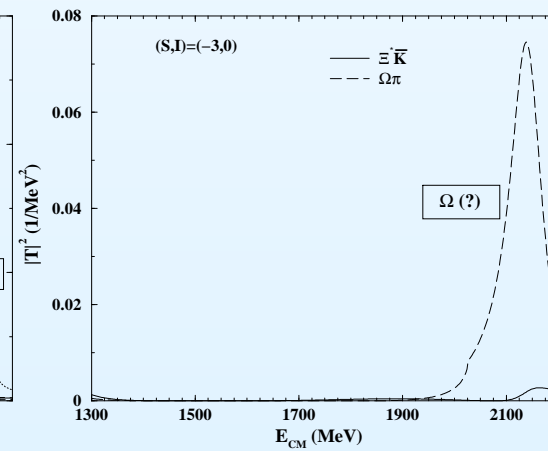
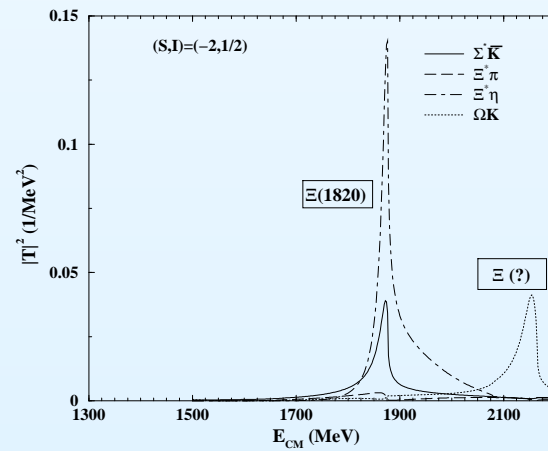
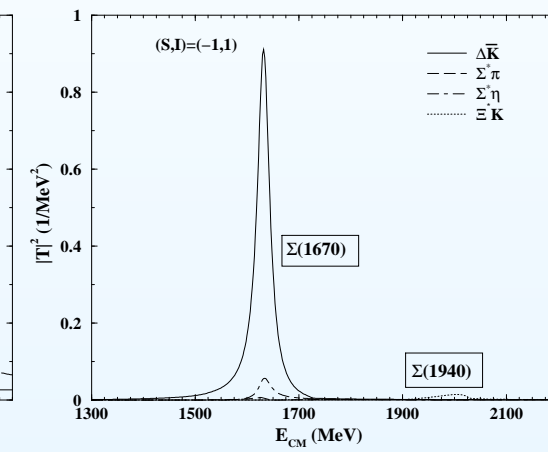
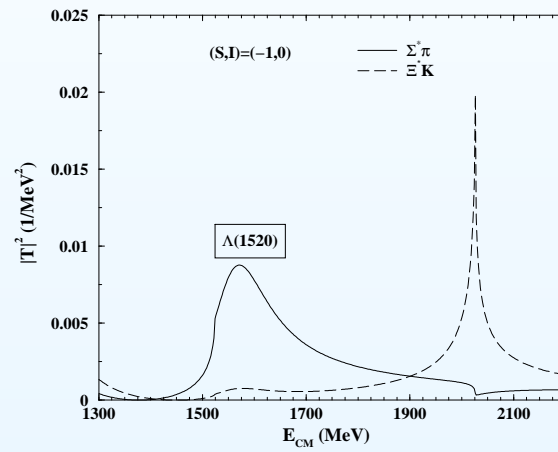
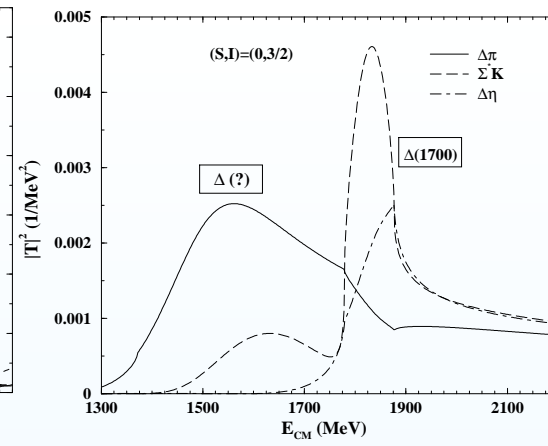
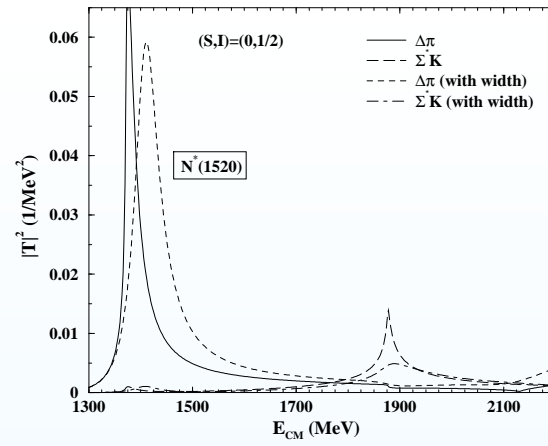
$$\mathcal{D}^\nu T_{abc}^\mu = \partial^\nu T_{abc}^\mu + (\Gamma^\nu)_a^d T_{dbc}^\mu + (\Gamma^\nu)_b^d T_{adc}^\mu + (\Gamma^\nu)_c^d T_{abd}^\mu \quad (2)$$

$$\Gamma^\nu = \frac{1}{2}(\xi \partial^\nu \xi^\dagger + \xi^\dagger \partial^\nu \xi) \quad (3)$$

$$\xi^2 = U = e^{i\sqrt{2}\Phi/f} \quad (4)$$

$$V_{ij} = -\frac{1}{4f^2} C_{ij} (k^0 + k'^0). \quad (5)$$

$$\begin{aligned} |\pi\Sigma^*; I=0\rangle &= \frac{1}{\sqrt{3}} |\pi^-\Sigma^{*+}\rangle - \frac{1}{\sqrt{3}} |\pi^0\Sigma^{*0}\rangle - \frac{1}{\sqrt{3}} |\pi^+\Sigma^{*-}\rangle \\ |K\Xi^*; I=0\rangle &= -\frac{1}{\sqrt{2}} |K^0\Xi^{*0}\rangle + \frac{1}{\sqrt{2}} |K^+\Xi^{*-}\rangle. \end{aligned} \quad (6)$$



Similar results obtained in Lutz and Kolomeitsev before in
Phys.Lett.B585:243-252,2004

Introduction of the $\bar{K}N$ and $\pi\Sigma$ channels

$\bar{K}N$ and $\pi\Sigma$ couple to $\pi\Sigma(1385)$ in D-wave

$$-it_{\bar{K}N \rightarrow \pi\Sigma^*} = -i\beta_{\bar{K}N} |\vec{k}|^2 \mathcal{C}(1/2 \ 2 \ 3/2; m, M - m) Y_{2, m-M}(\hat{k}) (-1)^{M-m} \sqrt{4\pi}. \quad (7)$$

$$-it_{\pi\Sigma \rightarrow \pi\Sigma^*} = -i\beta_{\pi\Sigma} |\vec{k}|^2 \mathcal{C}(1/2 \ 2 \ 3/2; m, M - m) Y_{2, m-M}(\hat{k}) (-1)^{M-m} \sqrt{4\pi}. \quad (8)$$

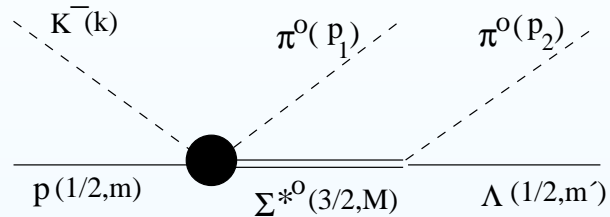
$$V = \begin{vmatrix} C_{11}(k_1^0 + k_1^0) & C_{12}(k_1^0 + k_2^0) & \gamma_{13} q_3^2 & \gamma_{14} q_4^2 \\ C_{21}(k_2^0 + k_1^0) & C_{22}(k_2^0 + k_2^0) & 0 & 0 \\ \gamma_{13} q_3^2 & 0 & \gamma_{33} q_3^4 & \gamma_{34} q_3^2 q_4^2 \\ \gamma_{14} q_4^2 & 0 & \gamma_{34} q_3^2 q_4^2 & \gamma_{44} q_4^4 \end{vmatrix}, \quad (9)$$

We chose a to get the pole at the physical position. β and γ chosen to reproduce the partial decay widths of the $\Lambda(1520)$ into $\bar{K}N(45\%)$ and $\pi\Sigma(42\%)$ and $\bar{K}N$ phase shifts.

From residues at pole $|g_{\pi\Sigma^*}| = 0.91$, $|g_{K\Xi^*}| = 0.29$, $|g_{\bar{K}N}| = 0.54$ and $|g_{\pi\Sigma}| = 0.45$.

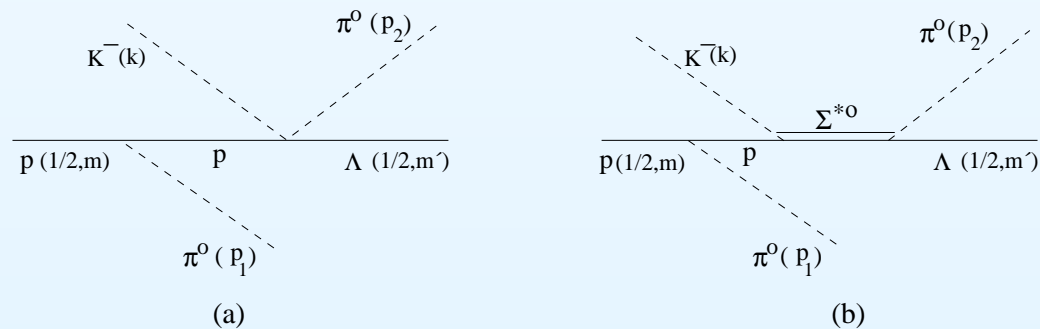
The reaction $K^- p \rightarrow \pi^0 \Sigma^{*0}(1385) \rightarrow \pi^0 \pi^0 \Lambda(1116)$

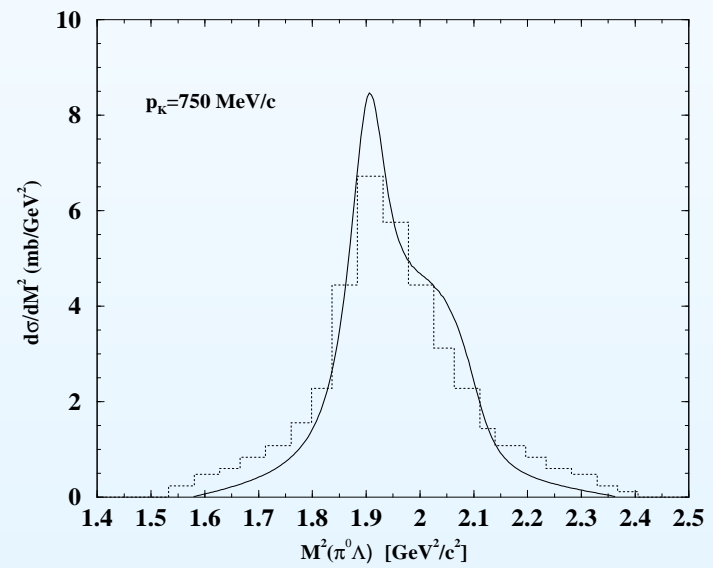
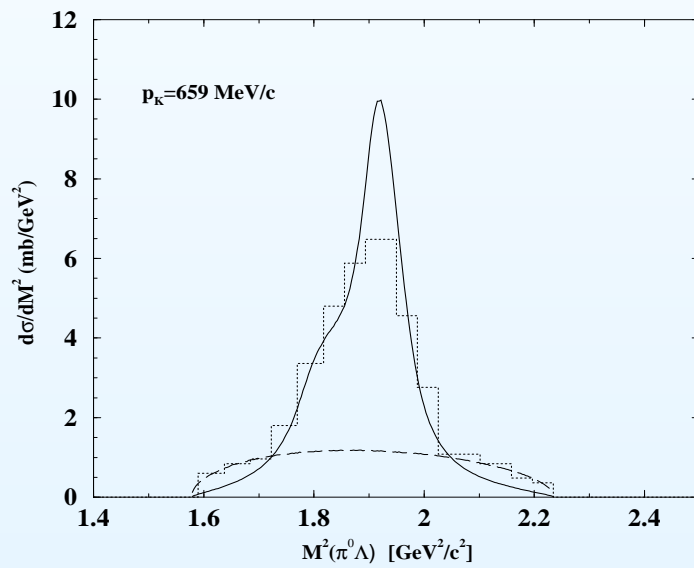
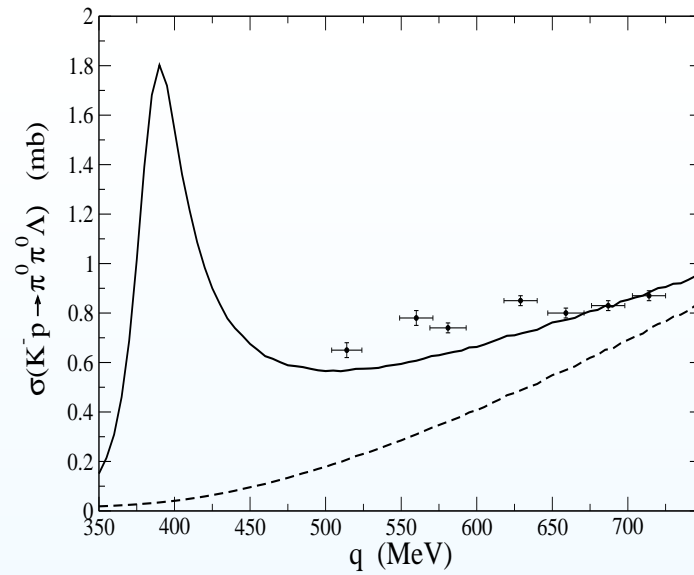
Prakhov...PRD04



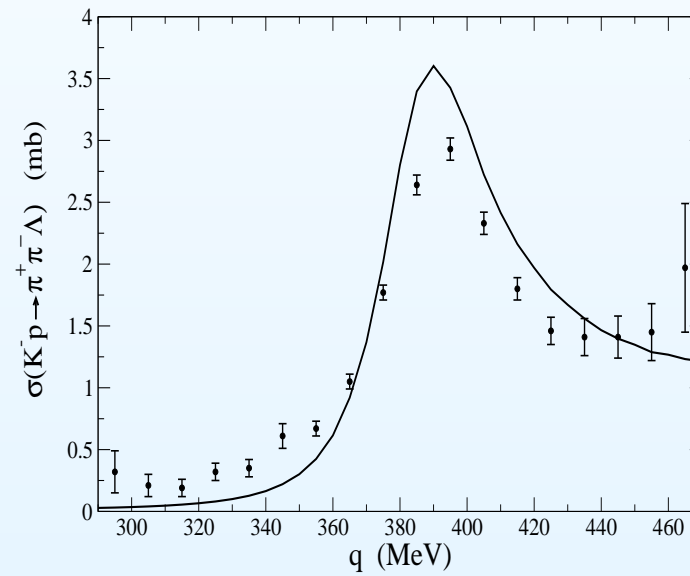
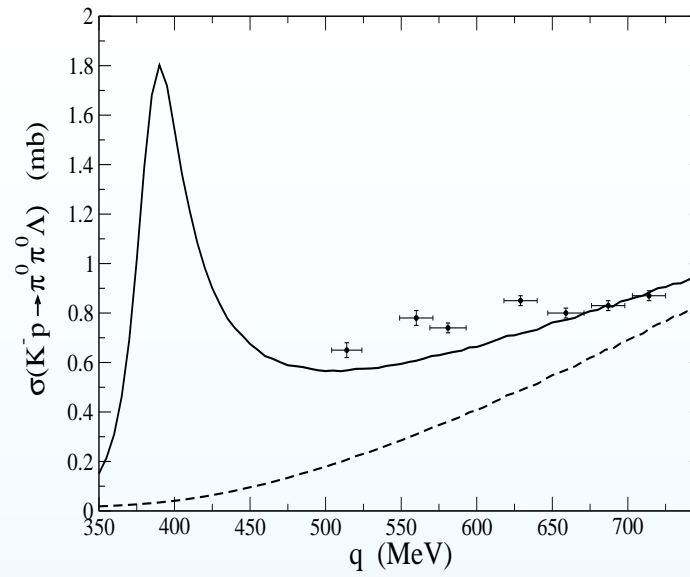
$$-it(\vec{p}_1, \vec{p}_2) = \frac{-iT_{\bar{K}N \rightarrow \pi \Sigma^*}}{3\sqrt{2}} \frac{f_{\Sigma^* \pi \Lambda} / m_\pi}{M_R - M_{\Sigma^*} + i\Gamma_{\Sigma^*} (M_R)/2} \left\{ \begin{array}{ll} -2p'_{2z} & m' = +1/2 \\ p'_{2x} + ip'_{2y} & m' = -1/2 \end{array} \right\}. \quad (10)$$

Conventional scheme for $K^- p \rightarrow \pi^0 \pi^0 \Lambda$





$K^- p \rightarrow \pi^0 \pi^0 \Lambda$, Prakhov,



$K^- p \rightarrow \pi^0 \pi^0 \Lambda$, Prakhov, $K^- p \rightarrow \pi^+ \pi^- \Lambda$, Mast

Hadrons in a nuclear medium

Talks of Mosel and Metag tuesday

Good review on the topic

M. Post, S. Leupold and U. Mosel , **Nucl. Phys. A 741 (2004) 81**

I present here examples closely linked to the chiral dynamics of the hadrons


- Kaons in a nuclear medium
- Kaon atoms
- η nuclear bound states
- $\Lambda(1520)$ in the medium
- Many body modes of \bar{p} annihilation

\bar{K} in a nuclear medium

One does many body corrections in the $\bar{K}N$ amplitude

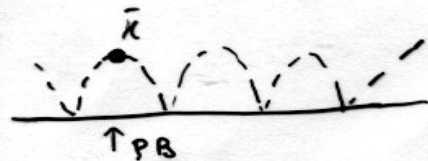
$$t(s) \rightarrow \tilde{t}(q, p)_{\substack{K \uparrow \\ N \uparrow}}$$

$$\Rightarrow \Pi_{\bar{K}}(q^0, q, p) = 2 \int \frac{d^3 p}{(2\pi)^3} n(\vec{p}) \left[\tilde{t}_{\bar{K}p}(q, p) + \tilde{t}_{\bar{K}n}(q, p) \right]$$



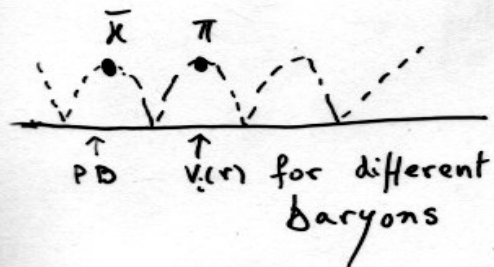
$$N \rightarrow \frac{1 - n(\vec{p})}{p^0 - E(p) + i\epsilon} + \frac{n(\vec{p})}{p^0 - E(p) - i\epsilon}$$

Pauli blocking Koch 94
 Waas, Weise 97
 shifts the $\Lambda(1405)$ at higher energies



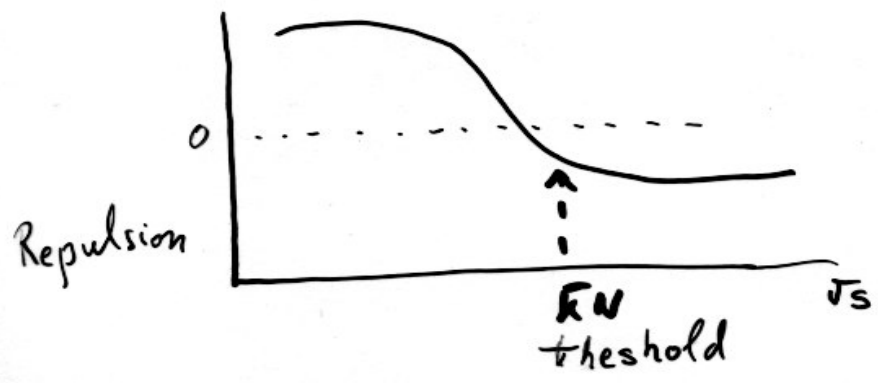
Selfconsistent use of \bar{K} selfenergy in the loops

Lutz 98
 Brings back the $\Lambda(1405)$ to the free position

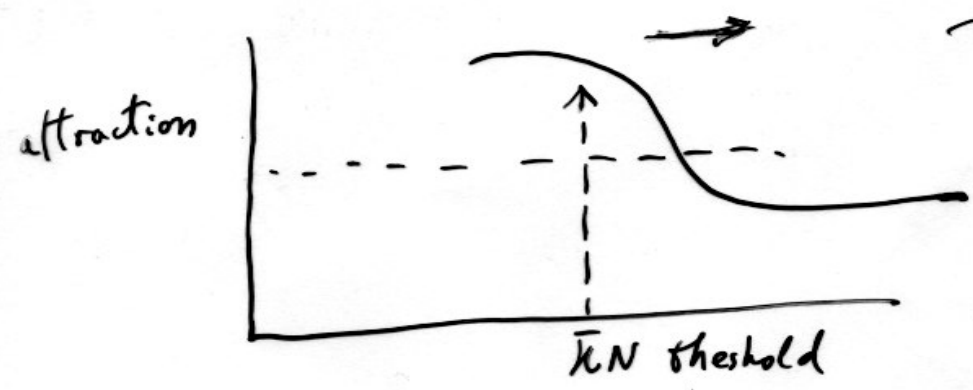


Selfcons. \bar{K} + π selfenergy + mean field baryon potential

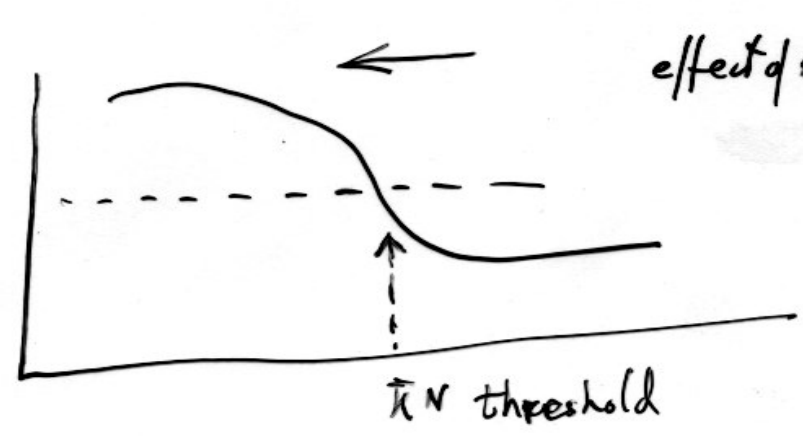
Ramos, E.O. NPA (2000)
 Opens new decay channels and widens spectral function



free case



Pauli blocking



effect of K^- attraction

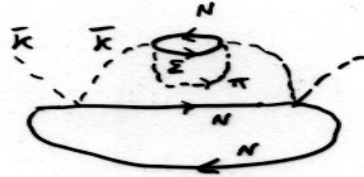
Medium decay channels

Koch
Waas, Weise



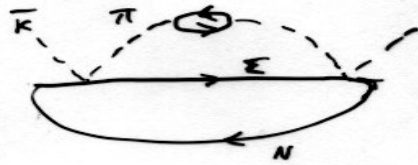
$$\bar{K} \Rightarrow (\Sigma h) \pi, (\Lambda h) \pi$$

Lutz



$$+ \bar{K} \rightarrow (\Sigma h)(p h) \pi, (\Lambda h)(p h) \pi$$

Ramos

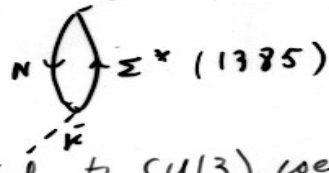
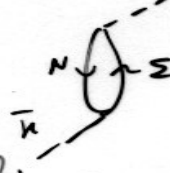
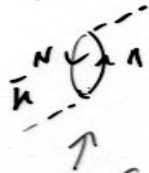


$$+ \bar{K} \rightarrow (\Sigma h)(p h), (\Lambda h)(p h)$$

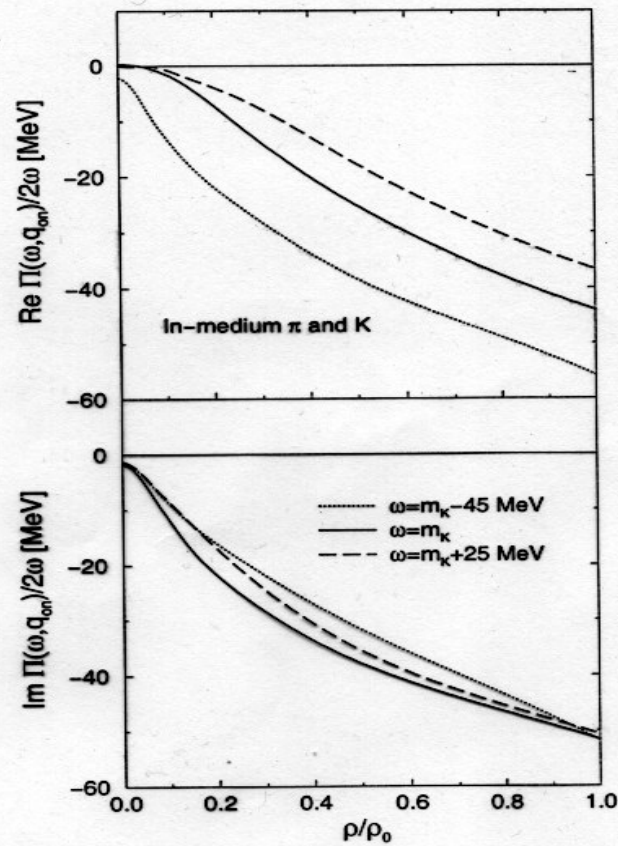


$$+ \text{extra } (\Sigma h)(p h) \pi, (\Lambda h)(p h) \pi$$

In addition we have p-wave \bar{K} selfenergy from Υh excitation



Couplings related to $SU(3)$ with D, F of original chiral lagrangian



Re V_{opt}

Im $V_{opt} \equiv -\frac{\Gamma}{2}$

FIG. 7. Real (top) and imaginary (bottom) parts of the K^- optical potential as a function of density obtained from the *In-medium pions and kaons* approximation. Results are shown for three different K^- energies: $\omega = m_K - 45$ MeV (dotted lines), $\omega = m_K$ (solid lines) and $\omega = m_K + 20$ MeV (dashed lines).

Similar results in
 Schaffner-Bielich, Koch, Effenberg
 Cieply, Friedman, Gal, Mares NPA 2000
 NPA 2001

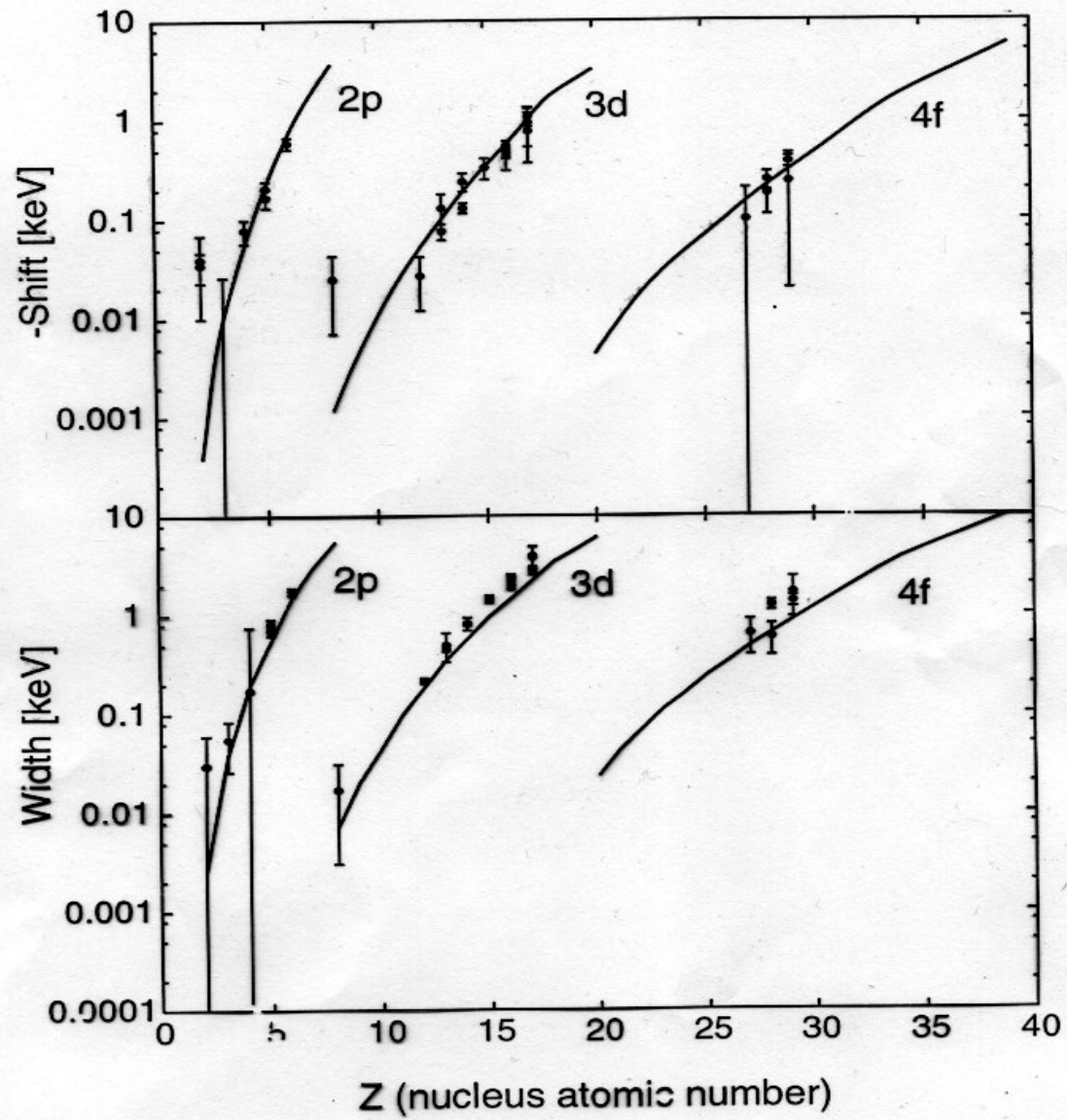
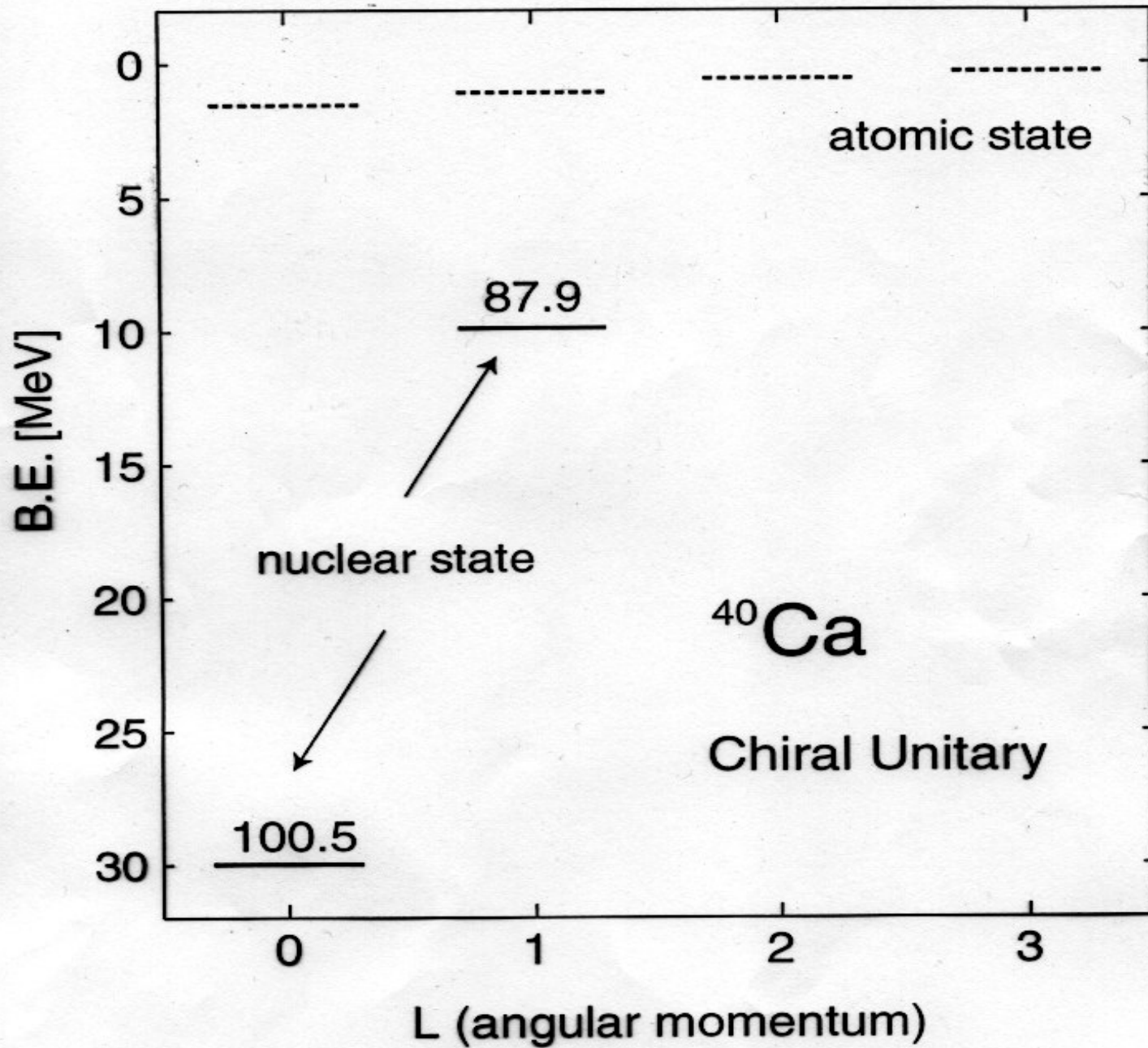


Fig.3

Improvements on the microscopic potential

Baca, Garcia Recio and Nieves show in NPA (2000) that the microscopic potential gives also good results for the rest of the available kaonic atom data.

They also add extra phenomenological terms and perform a best fit to the data, concluding that the extra terms amount to about 20 percent of the microscopic potential.



Short summary of deeply bound kaon atoms

1. Peaks seen at KEK in the p spectrum after K^- absorption in ${}^4\text{He}$ interpreted as deeply bound K atoms.
2. Broader peak seen at FINUDA in Λp invariant mass interpreted as a $K^- pp$ bound state.
3. Oset, Toki interpret KEK peaks as K^- absorption by nucleon pairs going to Σp and Λp and spectator daughter nucleus.
4. Magas, Ramos, Oset, Toki interpret FINUDA broad peak as rescattering of the p or the Λ following K^- absorption by nucleon pairs going to Λp .
5. New FINUDA paper in June 2006 on proton spectra, sees KEK like peaks in ${}^6\text{Li}$ and ${}^{12}\text{C}$ and interprets them with Oset, Toki mechanism of K^- absorption by pairs of nucleons.
6. Trento meeting on Hadron bound states... , June 2006, conclusions of the pannel discussion:
Present experiments do not provide any evidence of the existence of deeply bound K^- states.

η selfenergy in a nuclear medium

The procedure is like for kaons. Here one uses the same chiral lagrangian but the channels are

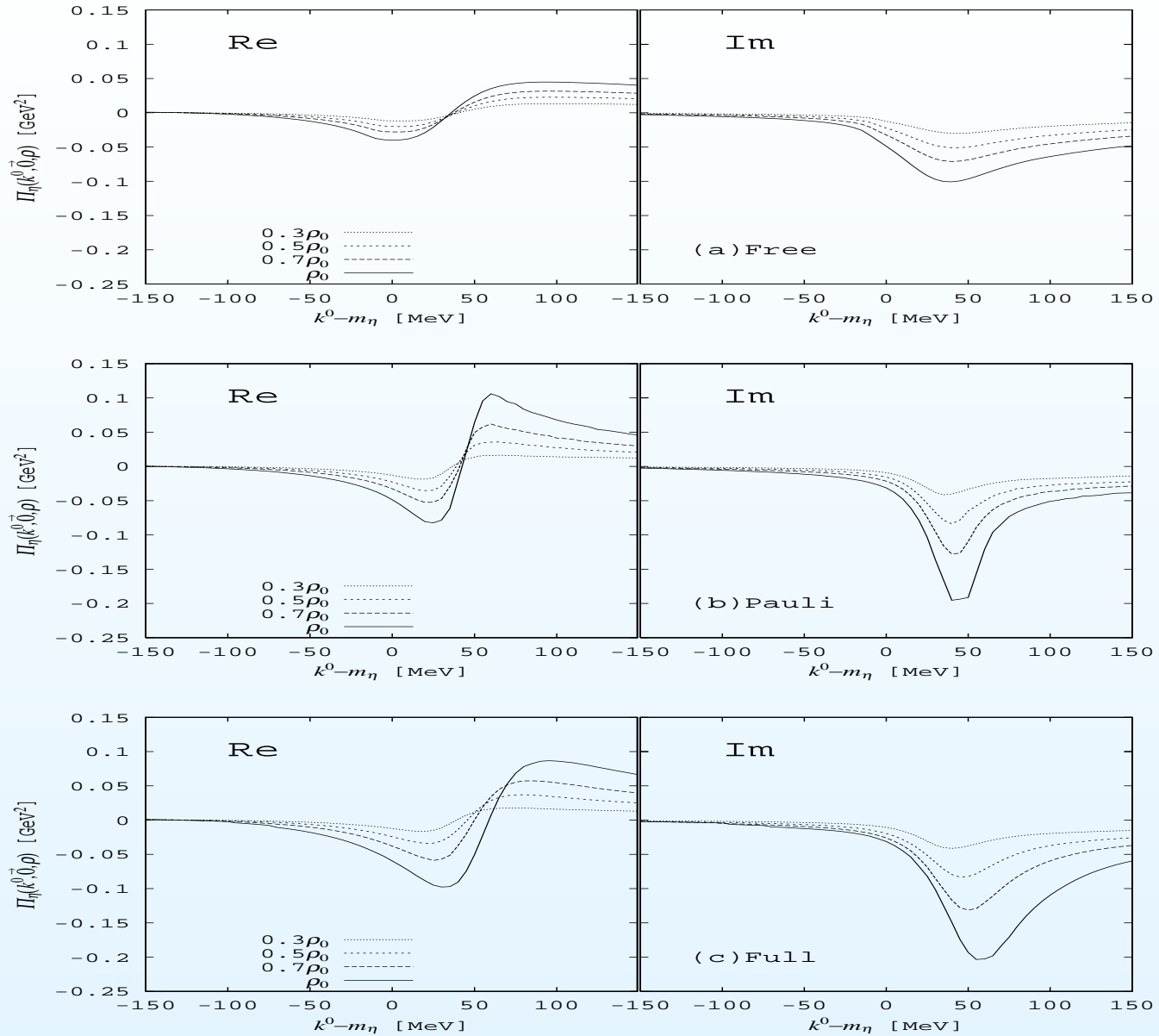
πN , ηN , $K\Lambda$, $K\Sigma$

One solves the coupled channel problem and obtains simultaneously

$\pi N \rightarrow \pi N$, $\pi N \rightarrow \eta N$, $\eta N \rightarrow \eta N$, etc

Working the many body in the $\eta N \rightarrow \eta N$ amplitude one obtains the η selfenergy in the nucleus.

Results



η self-energy for zero momentum, Top, (a) Free: the free space η - N amplitude. Middle, (b) Pauli. Bottom, (c) Full: both the Pauli blocking and hadron dressing.

η bound states

C. Garcia Recio, J. Nieves, T. Inoue and E. Oset, *Phys.Lett.B550 (2002) 47*

$$\left[-\vec{\nabla}^2 + \mu^2 + \Pi_\eta(\text{Re}[E], r) \right] \Psi = E^2 \Psi \quad (11)$$

Table 1: $(B, -\Gamma/2)$ for η -nucleus bound states calculated with the energy dependent potential.

	^{12}C	^{24}Mg	^{27}Al	^{28}Si	^{40}Ca	^{208}Pb
1s	(-9.71, -17.5)	(-12.57, -16.7)	(-16.65, -17.98)	(-16.78, -17.93)	(-17.88, -17.19)	(-21.25, -15.88)
1p			(-2.90, -20.47)	(-3.32, -20.35)	(-7.04, -19.30)	(-17.19, -16.58)
1d						(-12.29, -17.74)
2s						(-10.43, -17.99)
1f						(-6.64, -19.59)
2p						(-3.79, -19.99)
1g						(-0.33, -22.45)

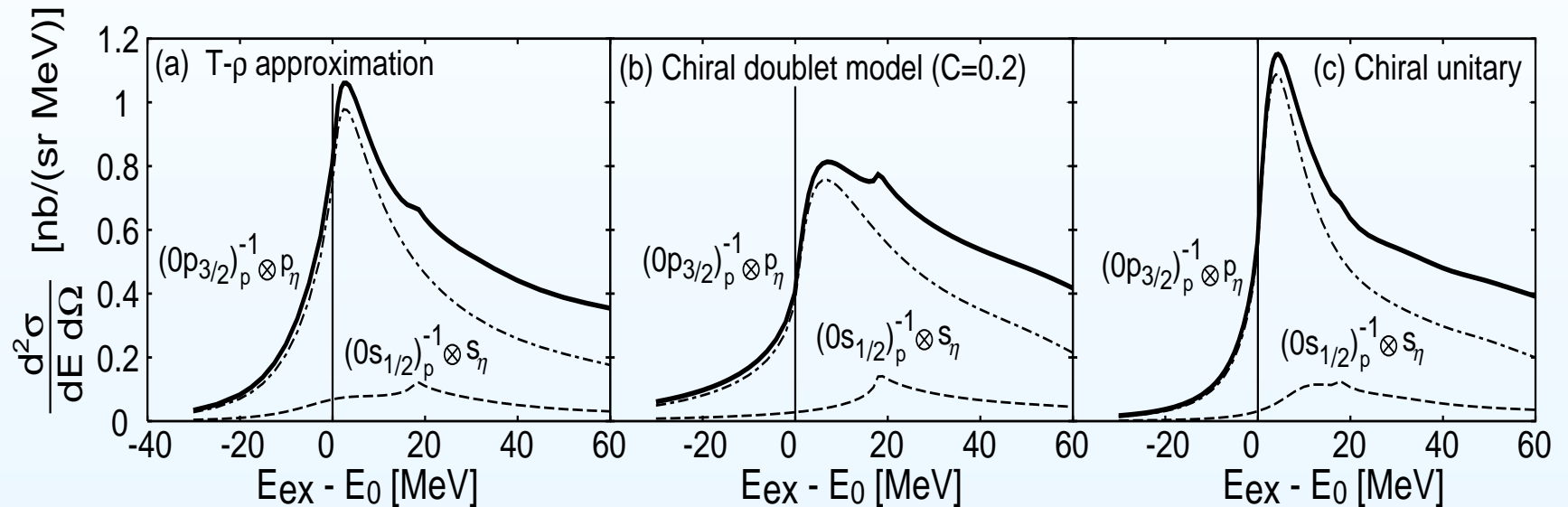
η bound states

Table 1: $(B, -\Gamma/2)$ for η -nucleus bound states calculated with the energy independent potential.

	^{12}C	^{24}Mg	^{27}Al	^{28}Si	^{40}Ca	^{208}Pb
1s	(-17.71, -25.42)	(-22.69, -25.78)	(-33.80, -30.63)	(-34.01, -30.36)	(-35.42, -30.12)	(-39.71, -28.65)
1p			(-5.28, -23.20)	(-6.07, -23.45)	(-13.02, -25.19)	(-31.97, -27.61)
1d						(-22.69, -26.30)
2s						(-19.11, -25.55)
1f						(-12.16, -24.69)
2p						(-6.81, -23.12)
1g						(-0.60, -22.74)

η bound states production

H. Nagahiro, D. Jido and S. Hirenzaki [Phys.Rev.C68:035205,2003](#)



Calculated spectra of $^{12}\text{C}(d, ^3\text{He})^{11}\text{B} \otimes \eta$ reaction at $T_d=3.5$ GeV as functions of the excited energy $E_{\text{ex}} - E_0$. E_0 is the η production threshold energy. The η -nucleus interaction is calculated by (a) the $t\rho$ approximation, (b) the chiral doublet model with $C = 0.2$, and (c) the chiral unitary approach. The total spectra are shown by the thick solid lines, and the dominant contributions from the $(0s_{1/2})_p^{-1} \otimes s_\eta$ and the $(0p_{3/2})_p^{-1} \otimes p_\eta$ configurations are shown by dashed lines and dash-dotted lines, respectively. Here, the proton-hole states are indicated as $(nl_j)_p^{-1}$ and η states as ℓ_η .

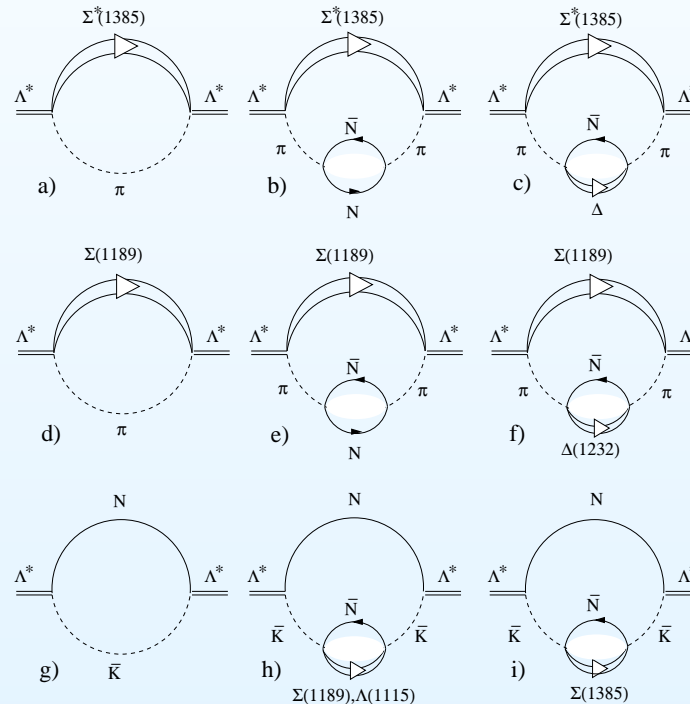
η bound states production

- Beware!! The peaks seen are not due to the bound states. They are consequence of the recoilless kinematics chosen to optimize the cross section. Spanning the energy range moves us from the magic recoilless kinematics and reduces the cross section, thus creating a peak structure which has nothing to do with the bound states.
- Note that in the case of the chiral doublet the interaction is repulsive and still one sees a peak in the production cross section.
- Moral: not everything that glitters is gold
- or equivalently
- not every peak is a signal of a bound state.

$\Lambda(1520)$ in the nuclear medium

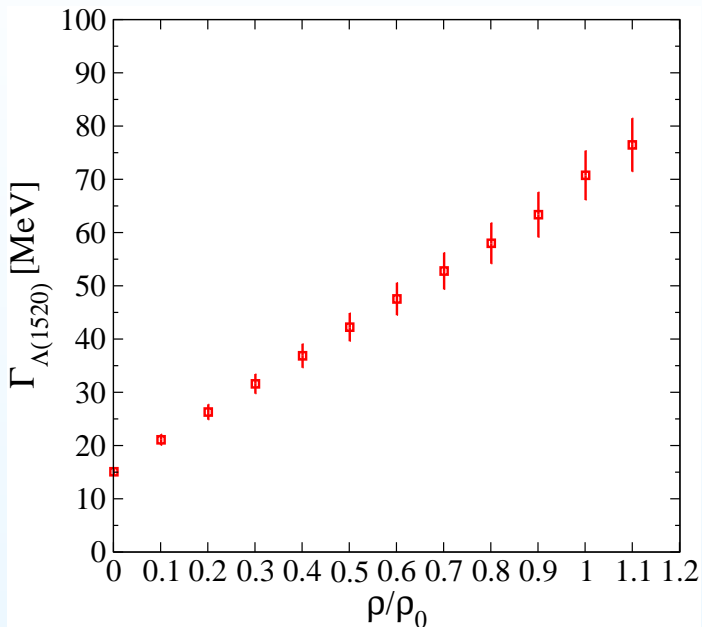
The coupling of the $\Lambda(1405)$ to $\pi\Sigma(1385)$ is very large but decay into this channel practically suppressed because of lack of phase space.

In nuclei a π can excite ph . Plenty of phase space. Large width.

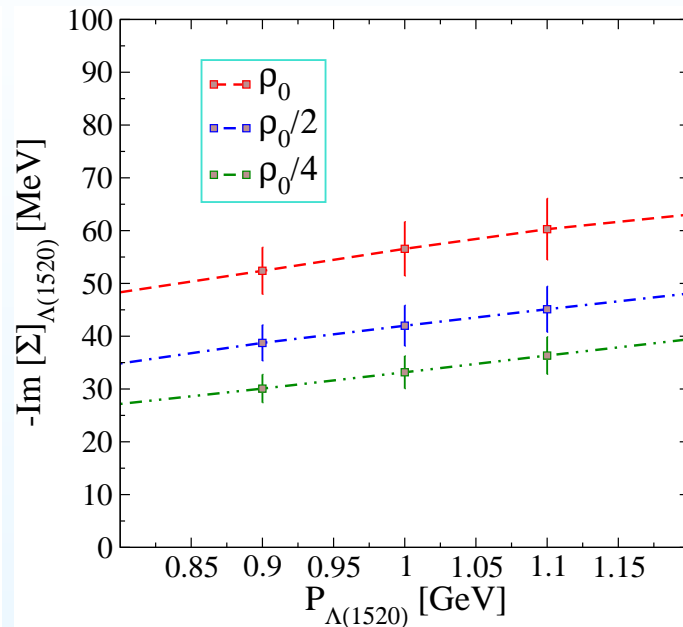


M.Kaskulov and E. O. , Phys Rev C (2006)

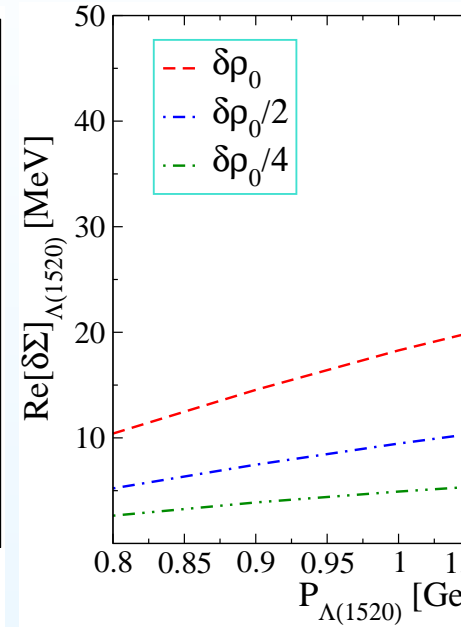
Results for $\Lambda(1520)$ in the nuclear medium



a)



b)



c)

These drastic changes could be observed experimentally suggestion made in [Kaskulov, Roca, E. O, Eur. Phys. J. A \(2206\)](#) by looking at the A dependence of the production cross section in

- proton induced $\Lambda(1520)$ production
- photon induced $\Lambda(1520)$ production (in progress at Spring8/Osaka)

MANY BODY MODES OF \bar{p} ANNIHILATION

low energy \bar{p}

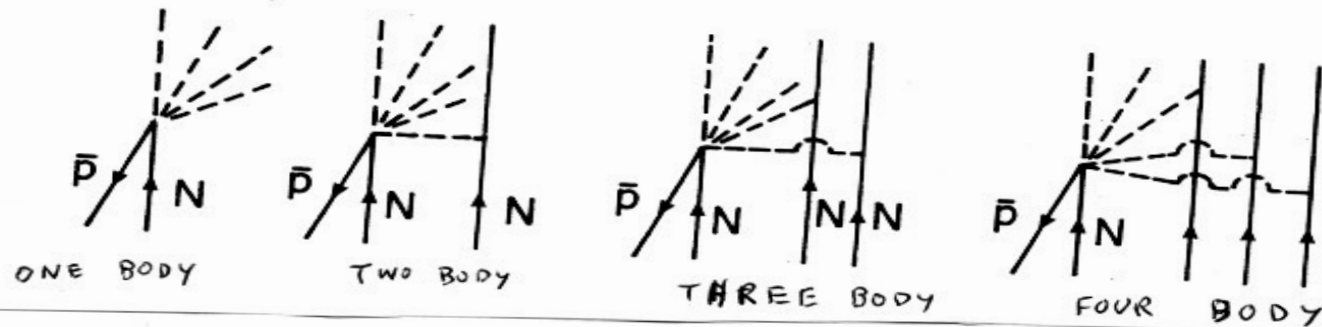


dominant decay

$$\langle n \rangle \sim 5$$

MANY BODY MODES OF ANNIHILATION IN NUCLEI

E. Hernández, E.O. NPA 493 (89)



$$P_{\text{anni}}^{(1)} = \sigma_{\text{anni}}(\bar{p}N \rightarrow \text{all}) \rho,$$

ONE BODY

$$P_{\text{anni}} = \sigma_{\text{anni}} \rho \left(1 + R \frac{\rho}{\rho_0} + S \left(\frac{\rho}{\rho_0} \right)^2 + T \left(\frac{\rho}{\rho_0} \right)^3 \right),$$

$$R = 4.59; \quad S = 10.6; \quad T = 12.8; \quad \text{at } T_p = 50 \text{ MeV},$$

$$R = 4.59; \quad S = 9.4; \quad T = 10.0; \quad \text{at } T_p = 175 \text{ MeV},$$

MANY BODY MODES OF \bar{p} ANNIHILATION
TESTED WITH \bar{p} PRODUCTION

E. HERNANDEZ, E.O
Z. PHYS A 341
(92)



$$\frac{d^2\sigma}{d\Omega dE(p)} = \int d^3r \frac{d^2\sigma_{\text{pro}}}{d\Omega dE(p)} \times \rho(r) e^{-\int_0^{\infty} P_{\text{anni}}(\rho(r'), E_p) dl}$$

$$D = \frac{1}{A} \int d^3r \rho(r) e^{-\int_0^{\infty} P_{\text{anni}}(\rho(r'), E_p) dl} \quad \bar{p} \text{ DISTORTION FACTOR}$$

		$D(1)$	$D(1+2)$	$D(1+2+3)$	$D(1+2+3+4)$
^{12}C ,	50 MeV	0.229	0.156	0.144	0.142
^{40}Ca ,	50 MeV	0.142	0.094	0.087	0.086
^{12}C ,	175 MeV	0.310	0.199	0.181	0.178
^{40}Ca ,	175 MeV	0.199	0.123	0.112	0.110

$$R' = D(1+2+3+4)/D(1),$$

$$\begin{aligned} R' &= 0.62 \quad \text{for } ^{12}\text{C} \quad \text{at } T_p = 50 \text{ MeV,} \\ R' &= 0.61 \quad \text{for } ^{40}\text{Ca} \quad \text{at } T_p = 50 \text{ MeV,} \\ R' &= 0.574 \quad \text{for } ^{12}\text{C} \quad \text{at } T_p = 175 \text{ MeV,} \\ R' &= 0.553 \quad \text{for } ^{40}\text{Ca} \quad \text{at } T_p = 175 \text{ MeV.} \end{aligned}$$

RELATIVE EFFECT
OF THE
2+3+4
body
annihilation
modes

$$2) \quad (p, \bar{p}) \quad pA \rightarrow \bar{p} + X$$

$$\frac{d^2\sigma}{d\Omega dE(\bar{p})} = \int d^3r e^{-\int_{-\infty}^z \sigma_{NN} \rho(\mathbf{b}, z') dz'} \\ \times \frac{d^2\sigma_{\text{pro}}}{d\Omega dE(\bar{p})} \rho(\mathbf{r}) e^{-\int_0^{\infty} P_{\text{ann}}(\rho(\mathbf{r}'), E_p) dl},$$

$R' = 0.71$ for ^{12}C at $T_p = 50$ MeV
and $\theta = 0^\circ$,

$R' = 0.73$ for ^{40}Ca at $T_p = 50$ MeV
and $\theta = 0^\circ$,

$R' = 0.66$ for ^{12}C at $T_p = 175$ MeV
and $\theta = 0^\circ$,

$R' = 0.69$ for ^{40}Ca at $T_p = 175$ MeV
and $\theta = 0^\circ$,

THE INITIAL P DISTORTION

MAKES THE REACTION MORE PERIPHERAL

AND THE MANY BODY MODES LESS

EFFECTIVE THAN IN (γ, \bar{p})

Conclusions

- Chiral dynamics is a powerful and ideal tool to face hadron interactions at intermediate energies in free space and in nuclei.
- It has shown as a side effect that some popular resonances qualify as dynamically generated or quasibound states of hadrons.
- It has predicted the existence on new resonances. Evidence for the second $\Lambda(1405)$ recently found.
- Chiral dynamics is important when dealing with hadrons in a nucleus.
- It makes prediction for kaon interaction with nuclei in good agreement with data of Kaon atoms. Predicts deeply bound kaon states but with a large width.
- striking medium effects in some resonances, like the $\Lambda(1520)$

Deeply bound kaon states

- The K^- optical potential on which predictions of narrow deeply bound K^- states was done is overly exaggerated and incomplete in the decay channels.
- The KEK and FINUDA experiment do not have any support for the interpretation of the data as bound kaons except the "theoretical predictions" of the mentioned work.
- We have shown that all the peaks can be interpreted in terms of K^- absorption on pairs of nucleons,
 - in KEK with remnant nucleus as spectator
 - in FINUDA, first peak with remnant nucleus as spectator
 - second peak with nuclear excitation to the continuum
- These mechanisms passed all tests for which there were available data.

Summary of DHD06 Workshop, Kyoto Feb 2006

- Akaishi strikes back, confusion of cut off in field theory and range of interaction. No selfconsistency yet, still $10\rho_0$ density.
- Yamazaki strikes back, makes wrong assumption on final state in $K^- \ ^4He$ absorption going to $p\Sigma \ nn$ instead of $p\Sigma \ d$ (small recoil energy of d , 10 MeV for 200 MeV/c of Fermi motion). Misses the experimental fact of the narrow signal in FINUDA for K^- absorption without extra final state interaction. Disguised offer of compromise, peaks partly from K^- absorption and partly from production of tribaryon. Compromise rejected: too much coincidence that the peaks appear in all nuclei at the K^- absorption kinematics.
- No help from any body else of the japanese community.
- No claims in the experimental talks about deeply bound kaon atoms. Back to tribaryon claim.
- Iwasaki pledge "please understand all this is still preliminary, we are working to understand what happens"
- The paper of 2003 with claims for deeply bound K from the K^- (*at rest*) absorption in $\ ^4He$, (K^-, n) has been withdrawn.

Summary of DHD06 Workshop, Kyoto Feb 2006

- Y. Yamagata presents calculations of (K^-, p) in flight and concludes that even if there are deeply bound kaon states the signal would be too weak to be seen in present experiments.
- S. Okada (Hayano exp.) presents results for $3d \rightarrow 2p$ X-rays of Kaonic Helium. 2p shift: Old experiments 40 eV, chiral unitary model 0.2 eV, Akaishi potential 11 eV. New experiment compatible with zero with 3-4 eV precision.